

# Ultralow-jitter, 1550-nm mode-locked semiconductor laser synchronized to a visible optical frequency standard

David J. Jones, Kevin W. Holman, Mark Notcutt, and Jun Ye\*

*JILA, National Institute of Standards and Technology and University of Colorado, Boulder, Colorado 80309-0440*

Juhi Chandalia, Leaf A. Jiang, and Erich P. Ippen

*Research Laboratory of Electronics, Massachusetts Institute of Technology, Cambridge, Massachusetts 02139*

H. Yokoyama

*Research Institute of Electrical Communication, Tohoku University, 2-1-1 Katahira, Aoba-ku, Sendai 980-8577, Japan*

Received December 6, 2002

Using high-bandwidth feedback, we have synchronized the pulse train from a mode-locked semiconductor laser to an external optical atomic clock signal and achieved what is to our knowledge the lowest timing jitter to date (22 fs, integrated from 1 Hz to 100 MHz) for such devices. The performance is limited by the intrinsic noise of the phase detector used for timing-jitter measurement. We expect such a highly stable device to play an important role in fiber-network-based precise time/frequency distribution. © 2003 Optical Society of America

OCIS codes: 320.7160, 120.3930, 140.5960.

A mode-locked laser diode (MLLD) provides a compact, reliable, and efficient source of an optical frequency comb in the 1.5- $\mu\text{m}$  wavelength region.<sup>1,2</sup> Such a source is attractive for the obvious reason of establishing frequency/wavelength reference grids for telecommunications. In light of recent developments of optical atomic clocks<sup>3,4</sup> and coherent optical spectrum synthesis,<sup>5</sup> MLLD-based comb systems can play a central role in clock signal distribution to remote sites. A low-jitter MLLD may also have important applications in ultrafast analog-to-digital conversion. The experimental approach that we are pursuing employs an ultrawide-bandwidth optical frequency comb generated by a mode-locked femtosecond Ti:sapphire laser that is phase locked to a highly stable, iodine-based optical frequency standard.<sup>4</sup> To establish optical phase coherence between the two systems, we will compare the optical second-harmonic output of a MLLD with the Ti:sapphire comb. The fundamental output of the MLLD at 1.5  $\mu\text{m}$  can be amplified and an extended bandwidth exceeding 200 nm can be produced with a continuum generation fiber.<sup>6</sup>

The first step toward these goals is to establish precise pulse repetition rate synchronization between the MLLD and the optical clock's Ti:sapphire laser comb. Fundamental (harmonic) hybrid mode locking is established when the external clock signal applied to the saturable-absorber section of the laser diode matches the exact (harmonic) value of the external-cavity mode spacing. Such MLLDs have produced timing jitter as small as 40 fs when the spectral noise is integrated from 10 Hz to 10 MHz.<sup>1,2</sup> The residual jitter is caused mainly by perturbation of the pulse train by the spontaneous quantum noise of the diode. Use of an intracavity filter restricts the pulse width (to 2–3 ps) and limits the amount of spontaneous-emission noise projected on the pulse to that within the pulse bandwidth, leading to smaller timing jitter. To further reduce the timing jitter, it becomes necessary to introduce a wide-bandwidth high-gain electronic feedback loop that

effectively replaces the original spontaneous quantum noise (within the servo bandwidth) with the (lower) measurement noise of the servo loop. In a manner similar to that used for stabilizing a cw laser diode by use of its injection current, we have built a multimegahertz-bandwidth servo loop to suppress the timing jitter in a MLLD. The feedback loop has made possible an order of magnitude of improvement over the performance of an injection-locked MLLD, with the residual timing jitter now limited by the intrinsic noise level of phase detectors used in generating the error signal.

Figure 1 shows the schematic diagram of the setup for stabilization and diagnosis of a MLLD. The optical clock signal is delivered by a mode-locked Ti:sapphire laser with a repetition rate of  $\sim 750$  MHz.<sup>7</sup> The comb spectrum of the Ti:sapphire laser, after it is broadened to an optical octave by an external microstructure fiber, is phase stabilized to a Nd:YAG laser, which is in turn frequency stabilized

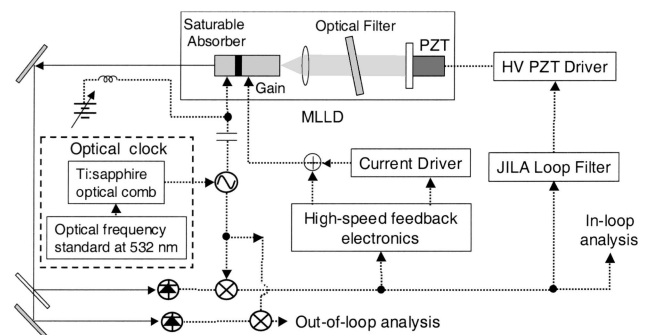


Fig. 1. Experimental configuration used to stabilize the timing jitter of a MLLD to an external clock signal derived from a mode-locked Ti:sapphire laser that is phase stabilized to an optical frequency standard. The output signal of the MLLD is phase-sensitively compared against the original clock signal by use of two doubly balanced low-noise mixers. The derived error signals are used for further noise reduction by a fast feedback loop as well as for out-of-loop noise analysis. HV, high-voltage.

to an iodine transition at 532 nm. The (in-)stability of the optical frequency standard is  $\sim 4 \times 10^{-14}$  at 1-s averaging time. The 8th harmonic of this optically derived radio-frequency (rf) signal at  $\sim 750$  MHz is used to injection lock the MLLD via its saturable absorber.

The repetition rate of the MLLD is  $\sim 5.98$  GHz (fundamentally mode locked). This frequency is set by the optical length of the external cavity, which contains a collimating graded-index lens, a 1-nm-bandwidth low-loss optical filter, and a high-reflecting (99.8%) mirror mounted on a piezo transducer. Variations of the diode bias current or the dc bias of the saturable absorber also significantly affect the MLLD repetition frequency. Hybrid mode locking is observed when the passively mode-locked repetition frequency is tuned to within the injection-locking range ( $\sim 10$  MHz) of the external clock signal. The output of the MLLD is detected by a fast photodiode and is phase-sensitively compared to the 8th harmonic of the master optical clock signal.<sup>7</sup> The error signal is then fed into a high-speed servo loop ( $\sim 5$ -MHz unity gain frequency) acting on the diode bias current, along with a slow servo acting to stabilize the external-cavity length of the MLLD. Although the in-loop error signal analysis provides useful information to characterize and improve the servo design, the out-of-loop measurement with an independent photodetector gives the ultimate check on the reliability of the stability transfer from the external clock to the MLLD. It is worth noting that, although the present work emphasizes only timing-jitter reduction, in future work to control the carrier-envelope phase of the pulses from the MLLD (to establish phase coherence), we can use the remaining control parameter, namely, the saturable absorber's bias voltage. The observed timing jitter must be significantly below an optical cycle ( $\sim 5$  fs at 1550 nm) over a given time scale for phase coherence to be observed within that time frame.

Figure 2 illustrates the detected rf spectrum of the fundamental repetition signal of the MLLD under various operating conditions. A large amount of phase noise near the carrier (associated with a free-running, passively mode-locked laser diode) was suppressed when the passive mode locking was aided by injection locking with an external clock signal, shown as the dotted data curve. A 200-kHz bandwidth feedback loop was employed first, with an external-cavity mirror piezoelectric transducer and the laser diode bias current through the current driver. The current driver limits the usable servo bandwidth. The phase noise near the carrier is further suppressed, but a visible servo noise bump near 200 kHz appears (solid curve, Fig. 2). A faster servo loop was implemented by establishment of a direct and physically short current feedback path between the phase detector that generates the error signal to the laser diode current-injection port. Only a passive phase-compensating filter network and a resistive attenuator were placed inside this fast current path. When this fast current loop was activated, the servo bump at 200 kHz was completely eliminated and replaced with a servo bump near 5 MHz. Although

the width of the carrier signal is not resolved by the resolution bandwidth of the rf spectrum analyzer, we can nevertheless witness enhanced amplitude of the carrier signal when this wide-bandwidth servo is turned on (triangles, Fig. 2).

Figure 3 summarizes the reduction of the timing jitter by the fast feedback loop based on controlling the diode injection current. We compare three cases, all under injection locking: without feedback, with feedback along with an in-loop noise analysis, and with noise analysis performed out of the feedback loop. Curves corresponding to the left-hand vertical axis give the measured timing-jitter spectral density, which we can integrate over a frequency range to determine the rms timing jitter within that spectral window, as indicated on the right-hand vertical axis in the figure. From the figure, the effect of the feedback is clearly manifested as noise reduction by approximately one order of magnitude over a Fourier frequency range extending from dc to  $\sim 100$  kHz. This effect is most

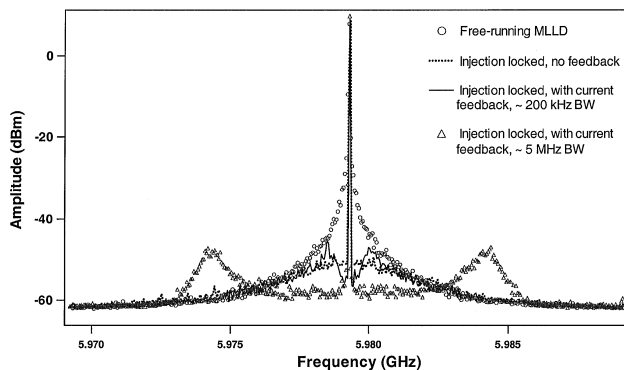


Fig. 2. Spectral analysis of the fundamental repetition signal of the MLLD under four operating conditions: free-running, passively mode locked; hybridly mode locked with injection of an external clock signal; hybridly mode-locked, with addition of a feedback loop of 200-kHz bandwidth; and with a 5-MHz bandwidth.

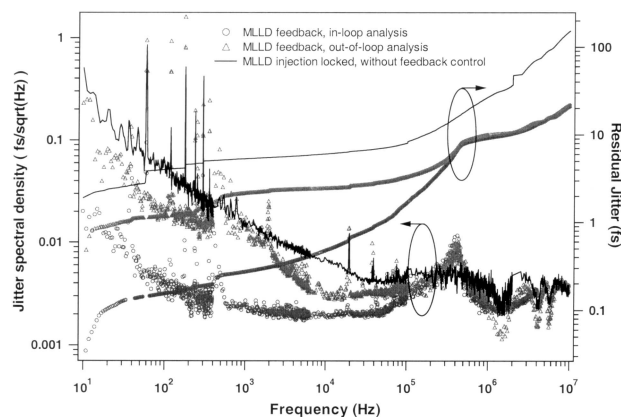


Fig. 3. Analysis of the timing-jitter Fourier spectral density of the MLLD under conditions of hybrid mode-locking with no feedback control, with feedback control but analyzed out of the loop and with feedback control and analyzed in loop. The residual rms jitter is integrated from 10 Hz up to an offset frequency from the 5.98-GHz carrier. The data are obtained with a fast Fourier transform spectrum analyzer (0.01–100 kHz) and a rf spectrum analyzer (0.1–10 MHz). The spikes are harmonics of line noise.

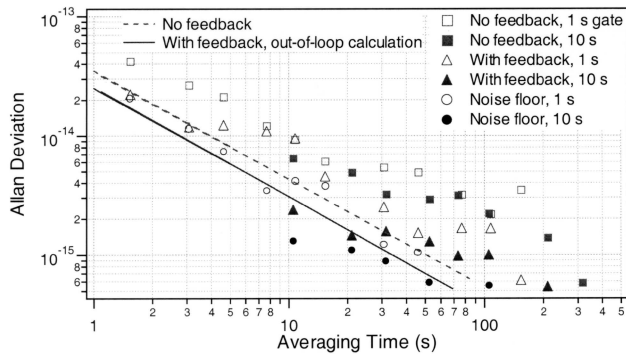


Fig. 4. Allan deviation analysis of the residual timing jitter. The calculated Allan deviation is determined from the jitter noise spectral density data displayed in Fig. 3. Direct frequency-counting results are shown by the symbols. Circles, measurement noise floor; squares, MLLD injection locked but without feedback; triangles, MLLD under feedback control.

clearly illustrated in the frequency range shown (10 Hz–10 MHz), where the integrated rms timing jitter is reduced ten times, from  $\sim 200$  to  $\sim 20$  fs, when the feedback loop is activated. From our data over a frequency range of 1 Hz to 100 MHz, the in-loop rms jitter was  $\sim 22$  fs. If too much gain is given to the 5-MHz loop (leading to a servo bump at that frequency, as shown in Fig. 2), even though there is greater noise reduction in the frequency range up to 1 MHz, the timing jitter actually increases. In the data shown in Fig. 3, the servo feedback was optimized for the lowest possible jitter. A true characterization of the performance of the stabilized MLLD requires noise analysis that is independent of the feedback loop. This out-of-loop analysis is carried out with an independent photodetector and associated microwave electronics. Of course, instabilities that are present in this independent detection loop cannot be distinguished from the MLLD noise. At low frequencies, the out-of-loop analysis is visibly noisier than the in-loop data. This difference can be attributed in large part to fiber-induced frequency noise of the out-of-loop fiber-coupled photodetector (which is differential noise compared with the first photodetector).

For frequency metrology applications, such as distribution of a highly stable clock signal by use of a MLLD, it is useful to compare the fractional frequency instabilities of the output signal of the MLLD with the original reference, with the fractional instabilities characterized by the Allan deviation.<sup>8</sup> The Allan deviation can be determined from the noise spectral density through the following expression:  $\sigma_y(\tau) = 2/\nu_0 \left\{ \int_{f_L}^{f_H} s_\phi(f) [\sin^4(\pi f \tau) / (\pi \tau)^2] df \right\}^{1/2}$ . Note that the timing-jitter spectral density shown in Fig. 3 corresponds (with a linear scaling factor) to the square root of the commonly defined phase noise spectral density,  $s_\phi(f)$ , in  $\text{rad}^2/\text{Hz}$ .  $\nu_0$  is the carrier frequency,  $\tau$  is the averaging time, and  $f_L$  ( $f_H$ ) is the lower (upper) bound of 10 Hz (10 MHz) for the integration. The calculated Allan deviations, obtained after curve fitting of the phase noise spectral

density to increase the frequency resolution for the integration, are shown in Fig. 4. To make a direct frequency comparison between the original and the regenerated clock signals, we have constructed a microwave interferometer<sup>9</sup> for single-sideband generation to shift one of the clock signals by 10 kHz. The heterodyne signal between the two clock signals is then at 10 kHz and can be counted with sufficient resolution. Allan deviations are determined from the juxtaposed frequency record. A 10-s gate time produces more accurate results than does a 1-s time since the counter has a finite dead time between counts. Data from the direct counting measurements are consistent with calculated results from the timing jitter spectra. The clock signal regenerated by the stabilized MLLD has a fractional instability within  $2.2 \times 10^{15}$  (relative to the original clock) at a 10-s averaging time.

In summary, using high-bandwidth feedback, we have stabilized a hybridly mode-locked semiconductor laser to an external, optically derived clock signal with high precision and reduced the timing jitter associated with the pulse repetition rate by approximately a factor of ten, leading to what is believed to be the lowest residual timing jitter achieved with a MLLD of  $\sim 22$  fs, integrated from 1 Hz to 100 MHz. This performance can be further improved if a narrower-bandwidth intracavity optical filter is used to more strongly limit the inherent jitter noise of the laser diode. We plan to use such a highly stable MLLD to distribute optical clock signals through a fiber network.

We thank J. L. Hall and J. Schlager for equipment loans. This work was supported by the Office of Naval Research, NASA, the U.S. Air Force Office of Scientific Research, the National Institute of Standards and Technology, and the National Science Foundation. K. W. Holman is a Hertz Foundation graduate Fellow. J. Chandalia is a Lucent Graduate Research Program for Women Fellow.

\*Corresponding author, ye@jila.colorado.edu.

## References

1. L. A. Jiang, M. E. Grein, E. P. Ippen, C. McNeilage, J. Searls, and H. Yokoyama, *Opt. Lett.* **27**, 49 (2002).
2. C. M. DePriest, T. Yilmaz, P. J. Delfyett, Jr., S. Etamad, A. Braun, and J. Abeles, *Opt. Lett.* **27**, 719 (2002).
3. S. A. Diddams, Th. Udem, J. C. Bergquist, E. A. Curtis, R. E. Drullinger, L. Hollberg, W. M. Itano, W. D. Lee, C. W. Oates, K. R. Vogel, and D. J. Wineland, *Science* **293**, 825 (2001).
4. J. Ye, L.-S. Ma, and J. L. Hall, *Phys. Rev. Lett.* **87**, 270801 (2001).
5. R. K. Shelton, L.-S. Ma, H. C. Kapteyn, M. M. Murnane, J. L. Hall, and J. Ye, *Science* **293**, 1286 (2001).
6. K. Imai, M. Kourogi, and M. Ohtsu, *IEEE J. Quantum Electron.* **34**, 54 (1998).
7. R. K. Shelton, S. M. Foreman, J. L. Hall, H. C. Kapteyn, M. M. Murnane, M. Notcutt, and J. Ye, *Opt. Lett.* **27**, 312 (2002).
8. D. W. Allan, *Proc. IEEE* **54**, 221 (1966).
9. E. N. Ivanov, M. E. Tobar, and R. A. Woode, *IEEE Trans. Ultrason. Ferroelectr. Freq. Control* **45**, 1526 (1998).